PROCEEDINGS OF SCIENCE

New measurement of $K^+ \to \pi^+ \nu\bar{\nu}$ branching ratio

Renato Fiorenza[a,*] **for the NA62 collaboration**[†]

[a] *INFN Sezione di Napoli*
Complesso universitario di Monte S. Angelo, ed. 6 – via Cintia, 80126, Napoli – Italy

E-mail: renato.fiorenza@cern.ch

The $K^+ \to \pi^+ \nu\bar{\nu}$ decay is a "golden mode" for flavour physics. Its branching ratio is predicted with high precision by the Standard Model to be less than 10^{-10}, and this decay mode is highly sensitive to indirect effects of new physics up to the highest mass scales. The NA62 experiment at the CERN SPS is designed to study the $K^+ \to \pi^+ \nu\bar{\nu}$ decay, and provided the world's most precise investigation of this decay using 2016–2018 data. Building on this success, the first results from a significantly improved analysis of new data, taken in 2021–2022 after beamline and detector upgrades, are presented, along with the combination with the 2016–2018 results.

The 43rd International Symposium on Physics in Collision (PIC2024)
22–25 October 2024
Athens, Greece

*Speaker

†A. Akmete, R. Aliberti, F. Ambrosino, R. Ammendola, B. Angelucci, A. Antonelli, G. Anzivino, R. Arcidiacono, M. U. Ashraf, T. Bache, A. Baeva, D. Baigarashev, L. Bandiera, M. Barbanera, V. Bautin, J. Bernhard, A. Biagioni, L. Bician, C. Biino, A. Bizzeti, T. Blazek, B. Bloch-Devaux, P. Boboc, V. Bonaiuto, M. Boretto, M. Bragadireanu, A. Briano Olvera, D. Britton, F. Brizioli, M.B. Brunetti, D. Bryman, F. Bucci, N. Canale, T. Capussela, J. Carmignani, A. Ceccucci, P. Cenci, M. Ceoletta, V. Cerny, C. Cerri, X. Chang, B. Checcucci, A. Conovaloff, P. Cooper, E. Cortina Gil, M. Corvino, F. Costantini, A. Cotta Ramusino, D. Coward, P. Cretaro, G. D'Agostini, J.B. Dainton, P. Dalpiaz, H. Danielsson, B. De Martino, M. D'Errico, N. De Simone, D. Di Filippo, L. Di Lella, N. Doble, B. Döbrich, F. Duval, V. Duk, D. Emelyanov, J. Engelfried, T. Enik, N. Estrada-Tristan, V. Falaleev, R. Fantechi, V. Fascianelli, L. Federici, S. Fedotov, A. Filippi, R. Fiorenza, M. Fiorini, M. Francesconi, O. Frezza, J. Fry, J. Fu, A. Fucci, L. Fulton, E. Gamberini, L. Gatignon, G. Georgiev, S. Ghinescu, A. Gianoli, R. Giordano, M. Giorgi, S. Giudici, F. Gonnella, K. Gorshanov, E. Goudzovski, C. Graham, R. Guida, E. Gushchin, F. Hahn, H. Heath, J. Henshaw, Z. Hives, E.B. Holzer, T. Husek, O. Hutanu, D. Hutchcroft, L. Iacobuzio, E. Iacopini, E. Imbergamo, B. Jenninger, J. Jerhot, R.W. Jones, K. Kampf, V. Kekelidze, C. Kenworthy, D. Kereibay, S. Kholodenko, G. Khoriauli, A. Khotyantsev, A. Kleimenova, M. Kolesar, A. Korotkova, M. Koval, V. Kozhuharov, Z. Kucerova, Y. Kudenko, J. Kunze, V. Kurochka, V. Kurshetsov, G. Lanfranchi, G. Lamanna, E. Lari, G. Latino, P. Laycock, C. Lazzeroni, G. Lehmann Miotto, M. Lenti, E. Leonardi, S. Lezki, P. Lichard, L. Litov, P. Lo Chiatto, R. Lollini, D. Lomidze, A. Lonardo, P. Lubrano, M. Lupi, N. Lurkin, D. Madigozhin, I. Mannelli, A. Mapelli, F. Marchetto, R. Marchevski, S. Martellotti, P. Massarotti, K. Massri, E. Maurice, M. Medvedeva, A. Mefodev, E. Menichetti, E. Migliore, E. Minucci, M. Mirra, M. Misheva, N. Molokanova, M. Moulson, S. Movchan, Y. Mukhamejanov, A. Mukhamejanova, M. Napolitano, R. Negrello, I. Neri, F. Newson, A. Norton, M. Noy, T. Numao, V. Obraztsov, A. Okhotnikov, A. Ostankov, S. Padolski, R. Page, V. Palladino, I. Panichi, A. Parenti, C. Parkinson, E. Pedreschi, M. Pepe, M. Perrin-Terrin, L. Peruzzo, L. Petit, P. Petrov, Y. Petrov, F. Petrucci, R. Piandani, M. Piccini, J. Pinzino, I. Polenkevich, C. Polivka, L. Pontisso, Yu. Potrebenikov, D. Protopopescu, M. Raggi, M. Reyes Santos, K. Rodriguez Rivera, M. Romagnoni, A. Romano, I. Rosa, P. Rubin, G. Ruggiero, V. Ryjov, A. Sadovsky, N. Saduyev, S. Sakhiyev, K. Salamatin, A. Salamon, C. Sam, J. Sanders, C. Santoni, G. Saracino, F. Sargeni, J. Schubert, S. Schuchmann, V. Semenov, A. Sergi, A. Shaikhiev, S. Shkarovskiy, M. Soldani, D. Soldi, M. Sozzi, T. Spadaro, F. Spinella, A. Sturgess, V. Sugonyaev, J. Swallow, A. Sytov, G. Tinti, A. Tomczak, S. Trilov, M. Turisini, P. Valente, T. Velas, B. Velghe, S. Venditti, P. Vicini, R. Volpe, M. Vormstein, H. Wahl, R. Wanke, V. Wong, B. Wrona, O. Yushchenko, M. Zamkovsky, A. Zinchenko.

 ISSN 1824-8039 . Published by SISSA Medialab.

PoS(PIC2024)047

1. The NA62 experiment

The $K^+ \to \pi^+\nu\bar{\nu}$ decay is described very precisely within the Standard Model (SM) and is highly sensitive to physics beyond the SM (BSM). It is short-distance dominated and suppressed by the GIM mechanism. Its SM branching ratio (BR) was predicted, using tree-level measurements of the CKM matrix elements, to be $\mathcal{B}(K^+ \to \pi^+\nu\bar{\nu}) = (8.4 \pm 1.0) \times 10^{-11}$ [1]. More recently, a calculation independent of $|V_{cb}|$ uncertainties led to the value $(8.60 \pm 0.42) \times 10^{-11}$ [2], while a different calculation using a full CKM parameter fit obtained $(7.86 \pm 0.61) \times 10^{-11}$ [3]; other recent predictions fall between these two [4–6]. The $K^+ \to \pi^+\nu\bar{\nu}$ decay can probe BSM physics at mass scales up to $O(100\,\text{TeV})$ [7]: significant deviations from the SM BR are predicted in several BSM scenarios, as well as correlations with the $K_L \to \pi^0\nu\bar{\nu}$ decay [8–16]. The latter decay is currently investigated by the KOTO experiment, which recently obtained a direct upper limit for its BR two orders of magnitude above the SM predictions [17].

NA62 is a fixed-target experiment at the CERN SPS, designed to study the $K^+ \to \pi^+\nu\bar{\nu}$ decay with a decay-in-flight technique. Data collected between 2016 and 2018 led to the measurement $\mathcal{B}(K^+ \to \pi^+\nu\bar{\nu}) = \left(10.6^{+4.1}_{-3.5}\right) \times 10^{-11}$ [18–20]. The following sections report about the result obtained with data collected between 2021 and 2022, and the combination with previous data: more details of the analysis can be found in [21].

The NA62 beamline and detector are described in [22]. The NA62 setup was upgraded for the 2021 data taking, and a sketch is shown in Figure 1. It features: a $75\,\text{GeV}/c$ unseparated hadron beam of 70 % π^+, 23 % p, 6 % K^+; a differential Cherenkov counter (KTAG) [23] with 70 ps time resolution; a silicon-pixel beam spectrometer (GTK) providing track momentum, direction and time measurements with resolutions of $0.15\,\text{GeV}/c$, 16 µrad, and 100 ps, respectively; veto detectors (VC, ANTI0, CHANTI) for activity associated with production of charged particles in the upstream region; a 65 m long fiducial volume (FV); a downstream magnetic spectrometer (STRAW) measuring momenta of charged secondary particles with resolution $\sigma_p/p = (0.30 \oplus 0.005 \cdot p/\text{GeV})$ %; a RICH for particle identification and timing with 70 ps resolution [24, 25]; scintillator hodoscopes (CHOD) used for trigger and timing purposes; an LKr electromagnetic calorimeter for both particle identification and photon veto; a muon veto system made of hadronic sampling calorimeters (MUV1,2), an iron wall, and an array of scintillator plates behind it (MUV3); a photon veto system (LAV, IRC, SAC) ensuring hermeticity up to 50 mrad from the beam axis.

The excellent performance of this detector [26–28], such as muon rejection of $O(10^7)$ and π^0 rejection of $O(10^8)$, is the foundation for a broad K^+ physics programme including precision chiral perturbation theory measurements [29–32], searches for lepton number and lepton flavour violations [33–37], searches for decays to invisible particles [38–41], and neutrino tagging [42]; the detector can be also used in a special *beam-dump mode* which allows for direct searches for new physics [43–45].

2. Data sample and selection

Data were collected in 2021 and 2022 at the design mean instantaneous intensity of 580 MHz, higher than the past. Dedicated trigger lines, denoted MB, NORM, PNN, are used to collect samples

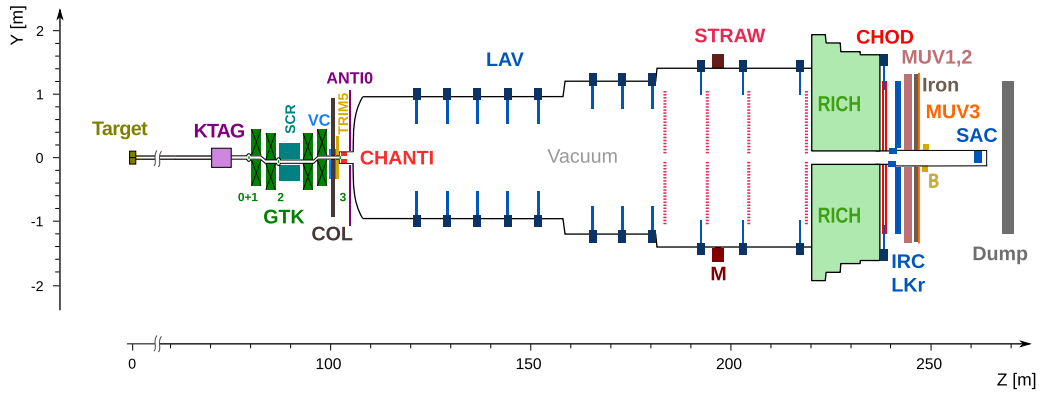

Figure 1: Schematic side view of the NA62 detector for data-taking from 2021 onwards.

of $K^+ \to \mu^+ \nu$ decays (for control purposes), $K^+ \to \pi^+ \pi^0$ decays (for normalization), and signal candidates, respectively.

Selection criteria common to the signal and the normalization sample include: presence of a single STRAW track; positive identification of a π^+ candidate and μ^+ rejection, using RICH, LKr and MUV information (also input to a BDT classifier); tagging of a candidate beam K^+ in the KTAG and in the GTK; association between the π^+ track and the K^+ track, based on spatial and timing information; veto conditions against interactions and decays upstream of the FV, based on the GTK, VC, ANTI0 and CHANTI, as well as a BDT classifier using spatial information from the K^+ and π^+ tracks. The signal selection also includes photon veto criteria, and multiplicity veto criteria rejecting partially reconstructed charged particles.

Kinematic regions are defined in terms of the squared missing mass $m^2_{\text{miss}} = (P_K - P_\pi)^2$ (where P_K and P_π are the 4-momenta of the K^+ and π^+ candidates) and p_{π^+} (the π^+ candidate momentum), using GTK and STRAW measurements: they are shown in Figure 2-left. They are: signal regions, R1 and R2; background regions, $K_{\mu 2}R$, $K_{2\pi}R$ and $K_{3\pi}R$, containing $K^+ \to \mu^+ \nu$, $K^+ \to \pi^+ \pi^0$ and $K^+ \to \pi^+ \pi^+ \pi^-$ decays, respectively; control regions, CR1, CR2, CRmu, CRmu2, CRmu3, CR3pi, CR3D, used to validate background estimates.

Normalization events are required to lie in CR1, $K_{2\pi}R$, or CR2; signal events are required to lie in R1 or R2.

3. Signal sensitivity

The analysis is performed in 5 GeV/c wide bins of p_{π^+} separately; in the following, summed or averaged values for the whole 2021–2022 dataset are reported.

The effective number of normalization events $N^{\text{eff}}_{\pi\pi} = (1.953 \pm 0.005) \times 10^8$ is calculated based on the number of normalization events observed, the downscaling factor applied to the NORM trigger line, and the background contamination of the normalization sample. The effective number of K^+ decays $N_K = (2.85 \pm 0.01) \times 10^{12}$ is calculated from $N^{\text{eff}}_{\pi\pi}$, the branching ratio of the normalization $K^+ \to \pi^+ \pi^0$, $\pi^0 \to \gamma\gamma$ decay chain, and the normalization selection acceptance $A_{\pi\pi} = (13.410 \pm 0.005)$ %, evaluated with simulations.

The single event sensitivity is $\mathcal{B}_{\rm SES} = (N_{\rm K} A_{\pi\nu\bar{\nu}} \varepsilon_{\rm trig} \varepsilon_{\rm RV})^{-1} = (8.48 \pm 0.29) \times 10^{-12}$, where: $A_{\pi\nu\bar{\nu}} = (7.62 \pm 0.22)$ % is the signal selection acceptance, evaluated with simulations; $\varepsilon_{\rm trig} = (85.9 \pm 1.4)$ % is the trigger efficiency ratio of the PNN and NORM trigger lines for the signal and normalisation samples, respectively; $\varepsilon_{\rm RV} = (63.2 \pm 0.6)$ % is the *random veto efficiency*, accounting for signal losses from the veto of unrelated activity. The random veto efficiency is measured from a data control sample of $K^+ \to \mu^+ \nu$ decays selected from the MB trigger; it depends only on the instantaneous beam intensity (Figure 2-right), and is therefore independent of p_{π^+}.

The number of SM signal events expected, assuming $\mathcal{B}^{\rm SM}_{\pi\nu\bar{\nu}} = 8.4 \times 10^{-11}$ as the SM BR, is $N^{\rm SM}_{\pi\nu\bar{\nu}} = \mathcal{B}^{\rm SM}_{\pi\nu\bar{\nu}} / \mathcal{B}_{\rm SES} = 9.91 \pm 0.34$.

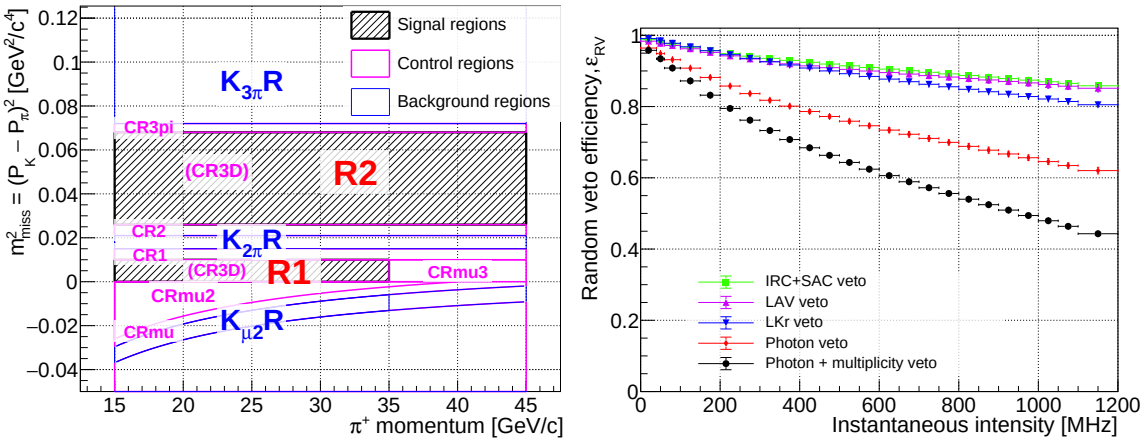

Figure 2: Left: definitons of kinematic regions in the $(p_{\pi^+}, m^2_{\rm miss})$ plane. The definitions of R1 and R2 include additional constraints on alternative measurements of the squared missing mass; CR3D is obtained by inverting such constraints, and overlaps them in this projection. Right: random veto efficiency as a function of the instantaneous beam intensity.

4. Backgrounds

Background from $K^+ \to \mu^+ \nu$, $K^+ \to \pi^+ \pi^0$ and $K^+ \to \pi^+ \pi^+ \pi^-$ decays in the FV arises from the non-gaussian tails of the $m^2_{\rm miss}$ resolution. For each of these decays, the background estimation is performed based on the number of events in the corresponding background region, and the reconstructed $m^2_{\rm miss}$ distribution, evaluated in dedicated control samples. Data-driven corrections are applied to account for specific classes of radiative $K^+ \to \mu^+ \nu\gamma$ and $K^+ \to \pi^+ \pi^0 \gamma$ decays which do not enter the control samples.

Background from $K^+ \to \pi^+ \pi^- e^+ \nu$ and $K^+ \to \pi^+ \gamma\gamma$ decays in the FV are estimated by using simulations. Other backgrounds from K^+ decays in the FV are estimated to be negligible.

The *upstream background* arises from decays and interactions upstream of the FV with misreconstruction or mismatching of the candidate π^+ downstream, which produces a fake reconstructed vertex. It is estimated with a fully data-driven strategy.

Background expectations are reported in Table 1. The comparison of expectation and observation in the control regions is shown in Figure 3-left, and validates the background expectations.

Further validation of the upstream background estimate is performed by using a set of statisically independent, upstream background-enriched, dedicated validation samples: results from this validation are shown in Figure 3-right.

Background	Events
$K^+ \to \pi^+\pi^0(\gamma)$	0.83 ± 0.05
$K^+ \to \mu^+\nu(\gamma)$	1.70 ± 0.47
$K^+ \to \pi^+\pi^+\pi^-$	0.11 ± 0.03
$K^+ \to \pi^+\pi^- e^+\nu$	$0.89^{+0.33}_{-0.27}$
$K^+ \to \pi^+\gamma\gamma$	0.01 ± 0.01
$K^+ \to \pi^0\ell^+\nu$	< 0.001
Upstream	$7.4^{+2.1}_{-1.8}$
Total	$11.0^{+2.1}_{-1.9}$

Table 1: Background expectations for 2021–2022 data.

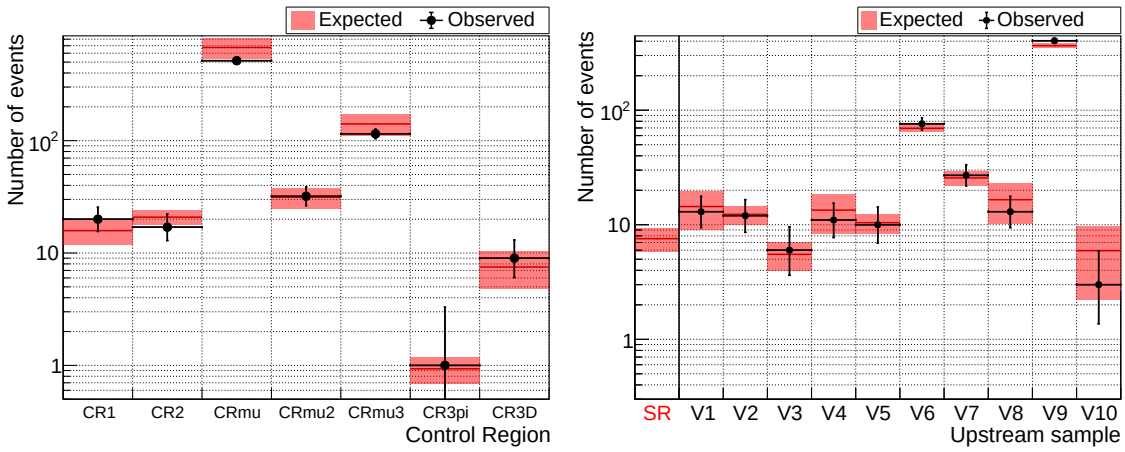

Figure 3: Left: expectations and observations in control regions. Right: expectations and observations in upstream background validation samples.

5. Results

After the signal selection, 6 events are observed in R1 and 25 in R2 (Figure 4-left).

Using the six π^+ momentum bins as independent categories and a profile likelihood ratio test statistic accounting for expectations of signal and backgrounds, the analysis of 2021–2022 data results in the measurement

$$\mathcal{B}(K^+ \to \pi^+\nu\bar{\nu})_{2021\text{–}2022} = \left(16.2^{+4.9}_{-4.3}\big|_{\text{stat}}\ ^{+1.4}_{-1.4}\big|_{\text{syst}}\right) \times 10^{-11} = \left(16.2^{+5.1}_{-4.5}\right) \times 10^{-11}\,.$$

These six categories are combined with the nine categories spanning 2016–2018 data [20] to obtain the measurement

$$\mathcal{B}(\mathrm{K}^+ \to \pi^+\nu\bar{\nu})_{2016\text{–}2022} = \left(13.0^{+3.0}_{-2.7}\big|_{\mathrm{stat}}\ ^{+1.3}_{-1.3}\big|_{\mathrm{syst}}\right) \times 10^{-11} = \left(13.0^{+3.3}_{-3.0}\right) \times 10^{-11}\,.$$

Observations and expectations in each of the resulting 15 categories are shown in Figure 4-right. With an expectation of 18^{+3}_{-2} background events and an observation of 51 events, the background-only hypothesis is rejected with a significance above 5σ, which marks the first observation of the $\mathrm{K}^+ \to \pi^+\nu\bar{\nu}$ decay. To date, this is the smallest branching ratio measured with a signal significance above 5σ.

The updated experimental and theoretical status is summarized in Figure 5. The $\mathcal{B}(\mathrm{K}^+ \to \pi^+\nu\bar{\nu})$ measurement precision has been improved from 40 % to 25 %; with more data to be analysed, NA62 aims to reach a precision better than 20 %.

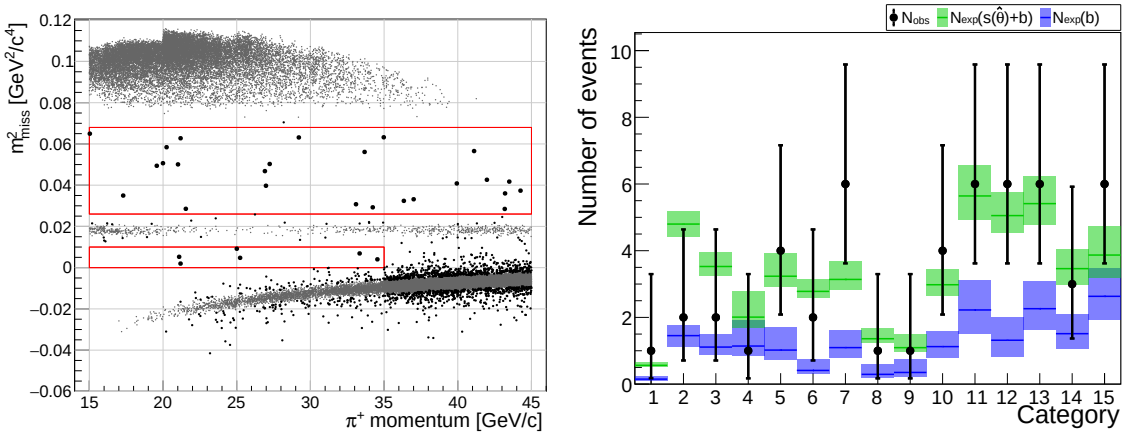

Figure 4: Left: distribution of events satisfying the signal selection in the $(p_{\pi^+}, m^2_{\mathrm{miss}})$ plane. Right: numbers of expected and observed events in the categories used for the statistical analysis of 2016–2022 data. Blue and green represent background and total (measured signal plus background) expectation, respectively.

References

[1] A.J. Buras, D. Buttazzo, J. Girrbach-Noe and R. Knegjens, *$K^+ \to \pi^+\nu\bar{\nu}$ and $K_L \to \pi^0\nu\bar{\nu}$ in the Standard Model: status and perspectives*, *JHEP* **11** (2015) 033 [1503.02693].

[2] A.J. Buras and E. Venturini, *The exclusive vision of rare K and B decays and of the quark mixing in the standard model*, *Eur. Phys. J. C* **82** (2022) 615 [2203.11960].

[3] G. D'Ambrosio, A.M. Iyer, F. Mahmoudi and S. Neshatpour, *Anatomy of kaon decays and prospects for lepton flavour universality violation*, *JHEP* **09** (2022) 148 [2206.14748].

[4] J. Brod, M. Gorbahn and E. Stamou, *Updated Standard Model Prediction for $K \to \pi\nu\bar{\nu}$ and ϵ_K*, *PoS* **BEAUTY2020** (2021) 056 [2105.02868].

[5] G. Anzivino et al., *Workshop summary: Kaons@CERN 2023*, *Eur. Phys. J. C* **84** (2024) 377 [2311.02923].

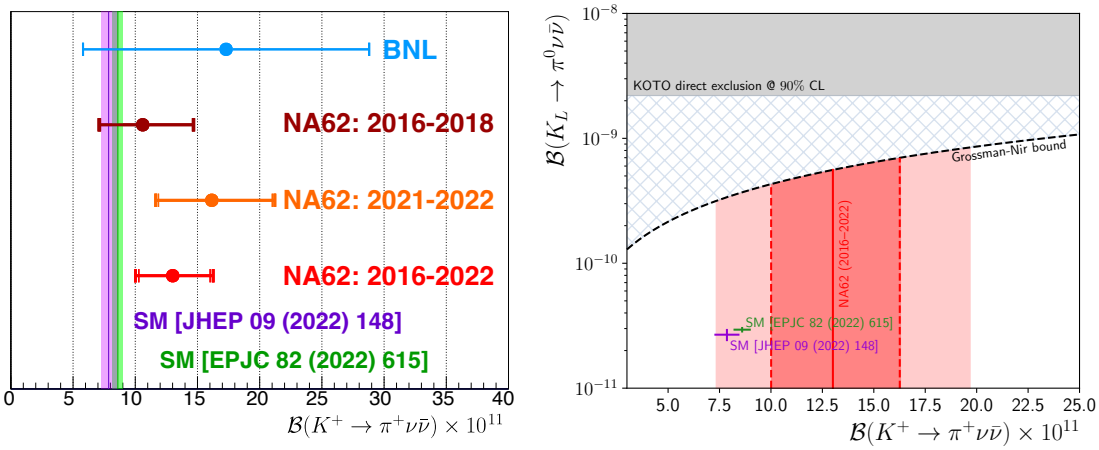

Figure 5: Left: history of $\mathcal{B}(K^+ \to \pi^+ \nu\bar{\nu})$ measurements [20, 21, 46] and recent SM predictions [2, 3]. Statistical and total uncertainties are shown by thinner and thicker vertical bars, respectively. Right: Status of $K \to \pi\nu\bar{\nu}$, including the Grossman-Nir bound [47], the SM predictions [2, 3], the most recent result from KOTO [17], and this result (dark and light areas represent 1σ and 2σ ranges, respectively).

[6] L. Allwicher, M. Bordone, G. Isidori, G. Piazza and A. Stanzione, *Probing third-generation New Physics with $K \to \pi\nu\bar{\nu}$ and $B \to K^{(*)}\nu\bar{\nu}$* , *Phys. Lett. B* **861** (2025) 139295 [2410.21444].

[7] A.J. Buras, D. Buttazzo and R. Knegjens, *$K \to \pi\nu\bar{\nu}$ and ε'/ε in simplified new physics models*, *JHEP* **11** (2015) 166 [1507.08672].

[8] C. Bobeth and A.J. Buras, *Leptoquarks meet ε'/ε and rare Kaon processes*, *JHEP* **02** (2018) 101 [1712.01295].

[9] M. Bordone, D. Buttazzo, G. Isidori and J. Monnard, *Probing Lepton Flavour Universality with $K \to \pi\nu\bar{\nu}$ decays*, *Eur. Phys. J. C* **77** (2017) 618 [1705.10729].

[10] J. Aebischer, A.J. Buras and J. Kumar, *Another SMEFT story: Z' facing new results on ϵ'/ϵ, ΔM_K and $K \to \pi\nu\bar{\nu}$*, *JHEP* **12** (2020) 097 [2006.01138].

[11] F.F. Deppisch, K. Fridell and J. Harz, *Constraining lepton number violating interactions in rare kaon decays*, *JHEP* **12** (2020) 186 [2009.04494].

[12] S. Descotes-Genon, S. Fajfer, J.F. Kamenik and M. Novoa-Brunet, *Implications of $b \to s\mu\mu$ anomalies for future measurements of $B \to K^{(*)}\nu\bar{\nu}$ and $K \to \pi\nu\bar{\nu}$*, *Phys. Lett. B* **809** (2020) 135769 [2005.03734]. Addendum: *Phys. Lett. B* **840** (2023) 137830.

[13] D. Marzocca, S. Trifinopoulos and E. Venturini, *From B-meson anomalies to Kaon physics with scalar leptoquarks*, *Eur. Phys. J. C* **82** (2022) 320 [2106.15630].

[14] Ò.L. Crosas, G. Isidori, J.M. Lizana, N. Selimović and B.A. Stefanek, *Flavor non-universal vector leptoquark imprints in $K \to \pi\nu\bar{\nu}$ and $\Delta F = 2$ transitions*, *Phys. Lett. B* **835** (2022) 137525 [2207.00018].

[15] M. Gorbahn, U. Moldanazarova, K.H. Sieja, E. Stamou and M. Tabet, *The anatomy of $K^+ \to \pi^+ \nu\bar{\nu}$ distributions*, *Eur. Phys. J. C* **84** (2024) 680 [2312.06494].

[16] A.J. Buras, J. Harz and M.A. Mojahed, *Disentangling new physics in $K \to \pi\nu\bar{\nu}$ and $B \to K(K^*)\nu\bar{\nu}$ observables*, *JHEP* **10** (2024) 087 [2405.06742].

[17] KOTO collaboration, *Search for the $K_L \to \pi^0 \nu\bar{\nu}$ Decay at the J-PARC KOTO Experiment*, arXiv:2411.11237.

[18] NA62 collaboration, *First search for $K^+ \to \pi^+ \nu\bar{\nu}$ using the decay-in-flight technique*, *Phys. Lett. B* **791** (2019) 156 [1811.08508].

[19] NA62 collaboration, *An investigation of the very rare $K^+ \to \pi^+ \nu\bar{\nu}$ decay*, *JHEP* **11** (2020) 042 [2007.08218].

[20] NA62 collaboration, *Measurement of the very rare $K^+ \to \pi^+ \nu\bar{\nu}$ decay*, *JHEP* **06** (2021) 093 [2103.15389].

[21] NA62 collaboration, *Observation of the $K^+ \to \pi^+ \nu\bar{\nu}$ decay and measurement of its branching ratio*, arXiv:2412.12015.

[22] NA62 collaboration, *The beam and detector of the NA62 experiment at CERN*, *JINST* **12** (2017) P05025 [1703.08501].

[23] NA62 collaboration, *Development of a new CEDAR for kaon identification at the NA62 experiment at CERN*, *JINST* **19** (2024) P05005 [2312.17188].

[24] G. Anzivino et al., *Precise mirror alignment and basic performance of the RICH detector of the NA62 experiment at CERN*, *JINST* **13** (2018) P07012 [1809.04026].

[25] G. Anzivino et al., *Light Detection System and Time Resolution of the NA62 RICH*, *JINST* **15** (2020) P10025 [2009.07581].

[26] NA62 collaboration, *Improved calorimetric particle identification in NA62 using machine learning techniques*, *JHEP* **11** (2023) 138 [2304.10580].

[27] NA62 collaboration, *Performance of the NA62 trigger system*, *JHEP* **03** (2023) 122 [2208.00897].

[28] I. Panichi et al. (NA62 collaboration), *High level performance of the NA62 RICH detector*, *Nucl. Instrum. Meth. A* **1045** (2023) 167583.

[29] NA62 collaboration, *A measurement of the $K^+ \to \pi^+ \mu^+ \mu^-$ decay*, *JHEP* **11** (2022) 011 [2209.05076]. Addendum: *JHEP* **06** (2023) 040.

[30] NA62 collaboration, *A study of the $K^+ \to \pi^0 e^+ \nu\gamma$ decay*, *JHEP* **09** (2023) 040 [2304.12271].

[31] NA62 collaboration, *Search for K^+ decays into the $\pi^+ e^+ e^- e^+ e^-$ final state*, *Phys. Lett. B* **846** (2023) 138193 [2307.04579].

[32] NA62 collaboration, *Measurement of the $K^+ \to \pi^+\gamma\gamma$ decay*, *Phys. Lett. B* **850** (2024) 138513 [2311.01837].

[33] NA62 collaboration, *Searches for lepton number violating K^+ decays*, *Phys. Lett. B* **797** (2019) 134794 [1905.07770].

[34] NA62 collaboration, *Search for lepton number and flavor violation in K^+ and π^0 decays*, *Phys. Rev. Lett.* **127** (2021) 131802 [2105.06759].

[35] NA62 collaboration, *Searches for lepton number violating $K^+ \to \pi^-(\pi^0)e^+e^+$ decays*, *Phys. Lett. B* **830** (2022) 132172 [2202.00331].

[36] NA62 collaboration, *A search for the $K^+ \to \mu^+ \nu e^+ e^+$ decay*, *Phys. Lett. B* **838** (2022) 137679 [2211.04818].

[37] NA62 collaboration, *First search for $K^+ \to \pi^0 \pi \mu e$ decays*, *Phys. Lett. B* **859** (2024) 139122 [2409.12981].

[38] NA62 collaboration, *Search for production of an invisible dark photon in π^0 decays*, *JHEP* **05** (2019) 182 [1903.08767].

[39] NA62 collaboration, *Search for heavy neutral lepton production in K^+ decays to positrons*, *Phys. Lett. B* **807** (2020) 135599 [2005.09575].

[40] NA62 collaboration, *Search for π^0 decays to invisible particles*, *JHEP* **02** (2021) 201 [2010.07644].

[41] NA62 collaboration, *Search for K^+ decays to a muon and invisible particles*, *Phys. Lett. B* **816** (2021) 136259 [2101.12304].

[42] NA62 collaboration, *First detection of a tagged neutrino in the NA62 experiment*, arXiv:2412.04033.

[43] NA62 collaboration, *Search for dark photon decays to $\mu^+\mu^-$ at NA62*, *JHEP* **09** (2023) 035 [2303.08666].

[44] NA62 collaboration, *Search for Leptonic Decays of Dark Photons at NA62*, *Phys. Rev. Lett.* **133** (2024) 111802 [2312.12055].

[45] NA62 collaboration, *Search for hadronic decays of feebly-interacting particles at NA62*, arXiv:2502.04241.

[46] E949 collaboration, *Study of the decay $K^+ \to \pi^+ \nu\bar{\nu}$ in the momentum region $140 < P_\pi < 199\,\mathrm{MeV}/c$*, *Phys. Rev. D* **79** (2009) 092004 [0903.0030].

[47] S. Navas et al. (Particle Data Group), *Review of Particle Physics*, *Phys. Rev. D* **110** (2024) 030001.